reported are those measured in the mixed solvents and are the same to within experimental error of those measured in CH_3CN/H_2O.
[14] In the absence of air, $[Os^{IV}(tpy)(Cl)(NH{=}CHCH_3)(NSC_6H_3Me_2)]^+$ does not undergo ligand substitution to form $[\mathbf{3C}]^+$ in CH_3CN/H_2O (1/1, v/v).
[15] a) M. A. Andrews, H. D. Kaesz, *J. Am. Chem. Soc.* **1979**, *101*, 7238–7244; b) M. A. Andrews, H. D. Kaesz, *J. Am. Chem. Soc.* **1979**, *101*, 7255–7259; c) M. A. Andrews, G. Vanbuskirk, C. B. Knobler, H. D. Kaesz, *J. Am. Chem. Soc.* **1979**, *101*, 7245–7254; d) M. A. Andrews, H. D. Kaesz, *J. Am. Chem. Soc.* **1979**, *101*, 7260–7264.
[16] S. G. Feng, J. L. Templeton, *J. Am. Chem. Soc.* **1989**, *111*, 6477–6478.
[17] W. Y. Yeh, C. S. Ting, S. M. Peng, G. H. Lee, *Organometallics*, **1995**, *14*, 1417–1422, and references therein.
[18] a) S. J. Anderson, F. J. Wells, G. Wilkinson, B. Hussain, M. B. Hursthouse, *Polyhedron* **1988**, *7*, 2615–2626; b) A. R. Barron, J. E. Salt, G. Wilkinson, M. Motevalli, M. B. Hursthouse, *J. Chem. Soc. Dalton Trans.* **1987**, 2947–2954; c) M. Bakir, P. E. Fanwick, R. A. Walton, *Inorg. Chem.* **1988**, *27*, 2016–2017.
[19] B. S. McGilligan, T. C. Wright, G. Wilkinson, M. Motevalli, M. B. Hursthouse, *J. Chem. Soc. Dalton Trans.* **1988**, 1737–1742.
[20] a) A. A. Sutyagina, T. V. Kulchitskaya, G. D. Vovchenko, *Sov. Electrochem.* **1975**, *11*, 1335–1337; b) A. A. Sutyagina, T. V. Kulchitskaya, T. L. Balabontseva, G. D. Vovchenko, *Vestn. Mosk. Univ. Ser. 2: Khim.* **1976**, *17*, 332–335.
[21] L. F. Rhodes, L. M. Venanzi, *Inorg. Chem.* **1987**, *26*, 2692–2695.
[22] J. March, *Advanced Organic Chemistry*, 3rd ed., Wiley Interscience, New York, **1985**, p. 809, and reference [1] on p. 815.
[23] H. Seino, Y. Tanabe, Y. Ishii, M. Hidai, *Inorg. Chim. Acta* **1998**, *280*, 163–171.
[24] a) J. J. R. F. Dasilva, M. F. C. G. Dasilva, R. A. Henderson, A. J. L. Pombeiro, R. L. Richards, *J. Organomet. Chem.* **1993**, *461*, 141–145; b) A. J. L. Pombeiro, D. L. Hughes, R. L. Richards, *J. Chem. Soc. Chem. Commun.* **1988**, 1052–1053; c) A. J. L. Pombeiro, *Inorg. Chim. Acta* **1992**, *200*, 179–186; d) A. J. L. Pombeiro, *New J. Chem.* **1994**, *18*, 163–174.
[25] The organic products from the reduction reactions were analyzed by GC-MS by using calibration curves and procedures similar to those found in ref. [12]. A typical product analysis is described in the Supporting Information.

The Ability of the α,α′-Diiminopyridine Ligand System to Accept Negative Charge: Isolation of Paramagnetic and Diamagnetic Trianions**

David Enright, Sandro Gambarotta,*
Glenn P. A. Yap, and Peter H. M. Budzelaar*

Recent work, both in this research group and elsewhere, has shown that the α,α′-diiminopyridine ligand [α,α′-{2,6-(*i*Pr)$_2$PhN=C(Me)}$_2$(C$_5$H$_3$N)], well known for its ability to form highly active polymerization catalysts,[1] can be involved in the organometallic transformations of metal centers. Alkylating agents may attack not only the imino function[2] but also all of the pyridine ring carbon atoms[3,4] and even the nitrogen atom.[5] In addition, dimerization may be achieved by imine reductive coupling[4] or by the cycloaddition of two pyridine rings to form a tricyclic system.[4] In parallel with all of these transformations, either one or both of the CH_3 groups attached to the imine functions may be partly deprotonated.[4,5] In this unusual variety of transformation, the metal center coordinated to the ligand may engage in redox reactions and may either lower or even increase its oxidation state.[3,6,7] This behavior illustrates the unique ability of this ligand system to a) accept negative charge with preferential spin-density localization on the imine groups and on the pyridine N and C_{para} atoms, and b) to engage in internal redox processes with the coordinated metal. The ability of the ligand to accept or to donate negative charge to the metal is paramount to the fine-tuning of the redox potential of the metal, and of its Lewis acidity which, in turn, determines the catalytic behavior of the metal complex.

Given the above scenario, we became interested in clarifying the ability of this remarkable ligand system to accept negative charge. For this purpose, we have carried out the reduction of [α,α′-{2,6-(*i*Pr)$_2$PhN=C(Me)}$_2$(C$_5$H$_3$N)] with strong reductants such as Li and [Li(naphthalenide)], in the absence of transition metals. Herein we describe our findings.

The reactions were carried out by treating a solution of [α,α′-{2,6-(*i*Pr)$_2$PhN=C(Me)}$_2$(C$_5$H$_3$N)] with either metallic Li under argon or [Li(naphthalenide)] under nitrogen in THF. Regardless of the stoichiometric ratio, the reduction with Li afforded a mixture of [α,α′-{2,6-(*i*Pr)$_2$PhN=C(Me)}$_2$-(C$_5$H$_3$N)][Li(thf)]$_3$ (**1**) and [{α-[2,6-(*i*Pr)$_2$PhN=C(Me)]}-{α′-[2,6-(*i*Pr)$_2$PhN-C(=CH$_2$)]}C$_5$H$_3$N][Li(thf)]$_2$[Li(thf)$_2$] (**2**) through a readily reproducible process. Both species contain a trianionic ligand (Scheme 1). Separation of the two extremely air-sensitive species was possible because of their relative solubilities in hexane. However, we observed that reactions carried out at low temperature with 3 equiv of [Li(naphthalenide)] afforded **2** as the only isolated compound (67%) and no evidence for the presence of **1**.

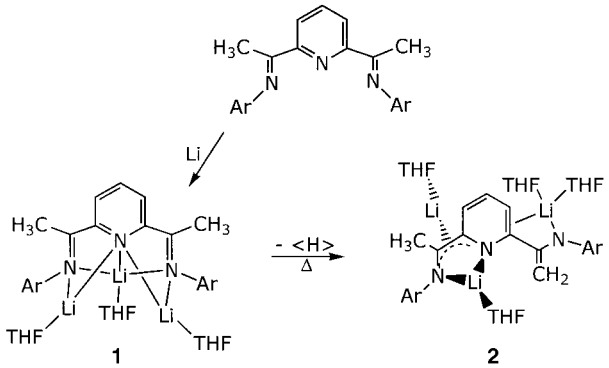

1 **2**

Scheme 1.

The connectivity of **1** was elucidated by an X-ray crystal structure (Figure 1). The complex contains the intact ligand, which adopts the usual chelating tridentate conformation

[*] Prof. S. Gambarotta, D. Enright, Dr. G. P. A. Yap
Department of Chemistry
University of Ottawa
Ottawa, Ontario, K1N 6N5 (Canada)
Fax: (+1) 613-5672-5170
E-mail: sgambaro@science.uottawa.ca.
Dr. P. H. M. Budzelaar
Department of Inorganic Chemistry
University of Nijmegen
Toernooiveld 1, 6525 ED Nijmegen (The Netherlands)
Fax: (+31) 24-355-3450
E-mail: budz@sci.kun.nl

[**] This work was supported by the Natural Sciences and Engineering Council of Canada (NSERC).

  0044-8249/02/4120-3873 $ 20.00+.50/0

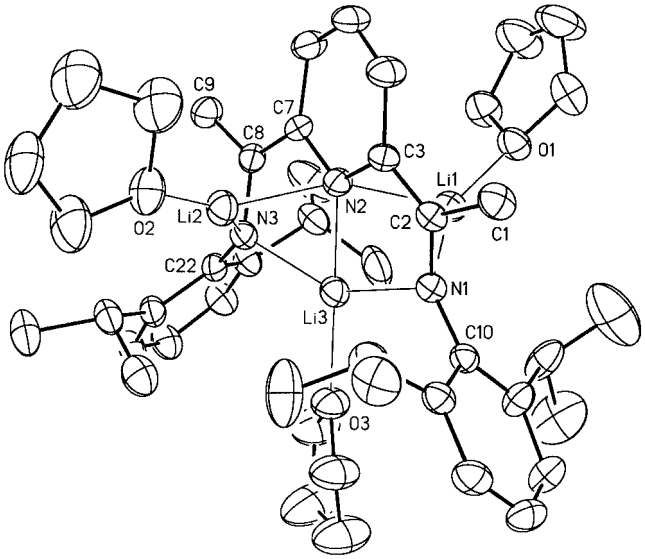

Figure 1. Thermal ellipsoid plot of **1**. Relevant bond lengths [Å] and angles [°]: C1-C2 1.522(4), C2-C3 1.373(4), C3-N2 1.421(4), C3-C4 1.481(4), C4-C5 1.407(5), C8-C9 1.512(4), Li3-N1 2.203(6), Li3-N2 1.993(6), Li3-N3 2.276(6), Li1-N1 1.994(6), Li1-N2 2.077(6), Li1-C2 2.138(6), Li2-C8 2.146(7), Li2-N2 2.049(6), Li2-N3 1.989(6); Li1-N2-Li2 154.6(3), Li3-N2-C3 119.1(3), Li3-N2-C7 121.2(2).

around the first Li atom which is, in turn, coordinated to one molecule of THF, with an overall distorted square-planar geometry. Two additional Li atoms, each solvated by one molecule of THF, are symmetrically placed on either side of the plane defined by the central Li atom and the three donor atoms. Each of these Li atoms is coordinated to a $N_{py}CCN_{im}$ fragment in a geometry reminiscent of metal–diene complexes. As a result, the pyridine N atom is pentacoordinated, and displays a near-regular trigonal bipyramidal geometry. The two out-of-plane Li atoms occupy a trigonal planar environment, with respect to the N and O donor atoms.

Complex **1** is a rare example of a paramagnetic organolithium complex that displays a magnetic moment ($\mu_{eff} = 1.30\ \mu_B$) which is lower than expected for a complex with one unpaired electron per molecule. The presence of antiferromagnetic exchange between the radical anions is a reasonable expectation. The ESR spectrum shows a single resonance peak at $g = 2.001$ with a hyperfine pattern appearing as a complex 25 line spectrum.

Density functional theory calculations (B3LYP)[8–11] on model complex **1a** (with the aryl substituents replaced by hydrogens) indicated the presence of a rather substantial SOMO–LUMO gap (approximately 2.3 eV) which accounts for the low-spin electronic configuration. The SOMO and HOMO are essentially identical to the LUMO and LUMO + 1 of the free ligand. Both orbitals (see Figure 2) are antibonding in the pyridine ring and between the C and N atoms of the imine moiety; the HOMO has substantial density at the N and C_{para} atoms of the pyridine moiety, whereas the SOMO has a nodal plane through these atoms. This behavior is in good agreement with the bond lengths displayed in the crystal structure, where the C–C bond formed between the *ortho* and *meta* C atoms are essentially single

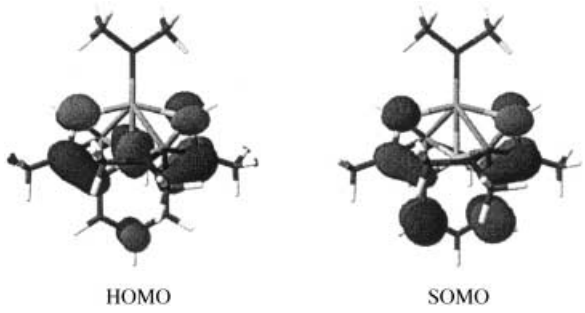

Figure 2. Pictorial drawing of the HOMO and SOMO of **1a**.

bonds whereas the C–C bonds formed by the *para* C atom are substantially shorter.

Although complex **2** originates from the same reaction and contains the same ligand skeleton, its structure is remarkably different. From the formal point of view it can also be regarded as a rare example of an organotrilithium complex. The loss of a proton from one of the methyl groups leads to the formation of a double bond with the adjacent C atom (Figure 3). The olefinic function is rotated approximately 30° out of the plane of the pyridine ring. One Li atom displays

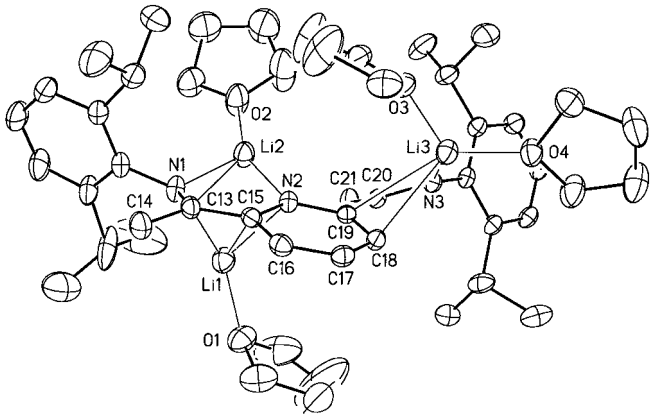

Figure 3. Thermal ellipsoid plot of **2**. Relevant bond lengths [Å] and angles [°]: C20-C21 1.366(4), C20-N3 1.364(3), C20-C19 1.526(4), C19-C18 1.374(4), C18-C17 1.442(4), C17-C16 1.352(4), C16-C15 1.446(4), C15-N2 1.451(4), C13-C15 1.394(4), C13-C14 1.514(4), Li1-N1 2.017(6), Li1-C13 2.156(6), Li1-C15 2.171(6), Li1-N2 2.121(6), Li2-N1 1.989(6), Li2-C13 2.779(6), Li2-N2 1.956(6), Li3-N3 1.958(5), Li3-C18 2.528(6), Li3-C19 2.754(6); C27-N3-Li3 129.7(2), C20-N3-Li3 110.(2), C20-N3-C27 118.4(2), C19-C20-C21 119.2(3), N3-C20-C21 128.1(3).

normal chelation to the iminopyridine moiety, while the second sits above the ring plane and binds to the $N_{py}CCN_{im}$ fragment in much the same way as the out-of-plane lithium atoms of **1**; both of these Li atoms are coordinated to one THF molecule. The third Li atom is σ-bound to the dangling enamide nitrogen atom and coordinated to two THF molecules. The pattern of bond lengths indicates substantial localization in the sense of the resonance structure depicted in Scheme 1.

The loss of a H atom from one of the two methyl groups of the imine carbon atom during the formation of **2** was conclusively demonstrated by NMR. The spectrum shows

  0044-8249/02/4120-3874 $ 20.00+.50/0

the presence of the two CH_2 protons at 2.04 and 3.01 ppm, coupled to each other and to the same carbon atom (66.39 ppm); their identity as CH_2 protons was confirmed from a DEPT experiment. The spectrum also displayed a remarkable upfield shift of the three pyridine resonances, two distinct phenyl rings, and two sets of *i*Pr groups.

In agreement with the observed diamagnetism of **2**, the conversion of **1** to **2** implies the loss of one hydrogen atom which corresponds to a formal one-electron oxidation. This might explain why a stronger reducing agent, such as metallic Li, is necessary for the formation of **1** while a milder reducing agent ([Li(naphthalenide)]) may favor the formation of **2**. In addition, the basicity of [Li(naphthalenide)] may play a role by promoting competition between reduction and hydrogen abstraction during its reaction with the free ligand. Finally, we have observed that **1** is thermally unstable and completely converts to **2** upon heating in toluene.

In conclusion, we have established that the popular [α,α′-{2,6-(*i*Pr)$_2$PhN=C(Me)}$_2$(C$_5$H$_3$N)] ligand can accommodate up to three electrons in the antibonding orbitals of the imino unit and the pyridine ring in a low-spin configuration. Assuming that upon alkylation similar metal-to-ligand charge-transfer also occurs in the transition-metal complexes formed with this ligand, the observed variety of transformations may be easily explained. The localization of spin density on the *meta* C atoms of the pyridine group explains the cycloaddition observed in the related Cr complex,[4] while the formation of a double bond explains the reductive coupling observed with Mn.[4,6] The charge localization at the *para* position of the pyridine ring accounts for both the lithiation[5a] and for the possibility of transferring alkyl groups directly from the metal center to any position of the pyridine ring.[3–5] What remains to be unveiled is how this ligand supports a high level of catalytic activity with various metals. The ability of the large π-system to accommodate negative charge might concurrently lead to increased Lewis acidity of the metal center, which has an obvious positive impact on catalytic performance. On the other hand, it may also help the stabilization of electron-rich, low-valent metals, as is often observed during the alkylation of these derivatives, and whose ability to promote polymerization is still controversial.[7]

Experimental Section

1: Freshly cut fragments of lithium foil (0.14 g, 21 mmol) were washed with hexanes, dried, and suspended in THF (100 mL). [α,α′-{2,6-(*i*Pr)$_2$PhN=C(Me)}$_2$(C$_5$H$_3$N)] (1.0 g, 2.1 mmol) was added to the reaction vessel. The mixture was stirred for 48 h under an argon atmosphere during which the color of the solution changed from light yellow to dark red/brown. Excess lithium was removed through a glass filter. THF was evaporated from the reaction mixture in vacuo without heating and the dark-brown residue was suspended in pentane (20 mL). Compound **2** was isolated as an insoluble, brown microcrystalline powder which was present even after filtration and additional washing with pentane (0.618 g, 38 %). The filtrate was concentrated to give a 15-mL solution and then cooled to −35 °C. Dark-red crystals of **1** (0.14 g, 0.2 mmol, 10 %) were isolated from the pentane solution. The extreme air-sensitivity of this compound, combined with the spontaneous loss of solvent, prevented any meaningful analytical data being obtained.

2: A solution of [Li(naphthalenide)] in THF (10 mL) was prepared by stirring a solution of naphthalene (0.8 g, 6.2 mmol) and freshly cut fragments of lithium foil (0.05g, 6.6 mmol). The resulting dark-green solution was diluted with additional THF (50 mL) and subsequently treated with [α,α′-{2,6-(*i*Pr)$_2$PhN=C(Me)}$_2$(C$_5$H$_3$N)] (1.0 g, 2.1 mmol). An instant color change from dark green to dark brown occurred. The reaction was stirred for an additional 10 min and the solvent was then removed in vacuo. The dry residue was left under dynamic vacuum overnight at room temperature to remove most of the naphthalene. The residual solid was then washed with cold pentane (30 mL), filtered, and isolated as an insoluble, brown diamagnetic powder (1.1 g, 1.4 mmol, 67 %). Crystals of **2** suitable for X-ray diffraction were grown by cooling a saturated solution in hexane to −35 °C. ^{1}H NMR (500 MHz, [D$_8$]THF, 23 °C): δ = 6.88 (2H, m; CH$_{(aromatic)}$); 6.75 (2H, m; CH$_{(aromatic)}$); 6.63 (1H, m; CH$_{(aromatic)}$); 6.36 (1H, m; CH$_{(aromatic)}$); 5.49 (1H, br s; CH$_{(pyridine)}$); 5.34 (1H, br s; CH$_{(pyridine)}$); 4.68 (1H, br s; CH$_{(pyridine)}$); 3.67 (12H, m; THF); 3.40 (4H, 2 overlapping septets; CH$_{(iPr)}$); 3.01 (1H, br s; CH$_2$); 2.04 (1H, br s; CH$_2$); 1.76 (12H, m; THF); 1.38 (3H, s, CH$_{(imino)}$); 1.19, 1.17, 1.09, 1.08 ppm (24H, 6 overlapping doublets; Me$_{(iPr)}$). ^{13}C NMR (125.72 MHz, [D$_8$]THF, 23 °C): δ = 167.52, 165.96, 157.98, 155.66, 154.80 (C$_{(quaternary)}$); 144.24, 143.82 (CH$_{(pyridine)}$); 123.01, 122.83, 119.76, 119.38, 115.38 (CH$_{(aromatic)}$); 114.35 (CH$_{(pyridine)}$); 112.66 (CH$_{(aromatic)}$); 108.31 (C$_{(quaternary)}$); 83.09 (CH$_{(pyridine)}$); 67.75 (THF); 66.39 (CH$_2$); 35.55, 32.57 (CH$_{(iPr)}$); 25.44 (THF); 24.99, 24.93, 24.50, 23.56 (Me$_{(iPr)}$).

Crystal data for **1**: C$_{45}$H$_{67}$N$_3$Li$_3$O$_3$, M_r = 718.84, monoclinic, space group *C*2/*c*, *a* = 21.2094(11), *b* = 11.5121(7), *c* = 37.855(2) Å, β = 103.279(2)°, *V* = 8995.7(9) Å^3, *Z* = 8, *T* = 233 K, F_{000} = 3128, *R* = 0.0789, *wR*^{2} = 0.2220, GOF = 1.043. **2**: C$_{49}$H$_{74}$N$_3$O$_4$Li$_3$, M_r = 789.93, monoclinic, space group *P*21/*c*, *a* = 15.0732(16), *b* = 18.855(2), *c* = 17.9425(19) Å, β = 105.170(2)°, *V* = 4921.6(9)Å^3, *Z* = 4, *T* = 203°K, F_{000} = 1720, *R* = 0.0759, *wR*^{2} = 0.1971, GOF = 1.067. CCDC-189630 and -189631 contain the supplementary crystallographic data for this paper. These data can be obtained free of charge via www.ccdc.cam.ac.uk/conts/retrieving.html (or from the Cambridge Crystallographic Data Centre, 12, Union Road, Cambridge CB2 1EZ, UK; fax: (+44) 1223-336-033; or deposit@ccdc.cam.ac.uk).

Received: July 11, 2002 [Z19715]

[1] a) G. J. P. Britovsek, M. Bruce, V. C. Gibson, B. S. Kimberley, P. J. Maddox, S. Mastroianni, S. J. McTavish, C. Redshaw, G. A. Solan, S. Strömberg, A. J. P. White, D. J. Williams, *J. Am. Chem. Soc.* **1999**, *121*, 8728; b) B. L. Small, M. Brookhart, *Polymer Prepr. Am. Chem. Soc. Div. Polym. Chem.* **1998**, *39*, 213; c) A. M. A. Bennett, DuPont, WO 98/27124 **1998** [*Chem. Abstr.* **1998**, *129*, 122973x]; d) A. M. A. Bennett, *CHEMTECH* **1999**, *29(7)*, 24.

[2] M. Bruce, V. C. Gibson, C. Redshaw, G. A. Solan, A. J. P. White, D. J. Williams, *Chem. Commun.* **1998**, 2523.

[3] D. Reardon, F. Conan, S. Gambarotta, G. P. A. Yap, Q. Wang, *J. Am. Chem. Soc*, **1999**, *121*, 9318.

[4] H. Sugiyama, G. Aharonian, S. Gambarotta, G. P. A. Yap, P. H. M. Budzelaar, *J. Am. Chem. Soc.*, in press.

[5] a) I. Korobkov, S. Gambarotta, G. P. A. Yap, P. H. M. Budzelaar, *Organometallics*, in press; b) G. K. B. Clentsmith, V. C. Gibson, P. B. Hitchcock, B. S. Kimberly, C. W. Rees, *Chem. Commun.* **2002**, 1498.

[6] D. Reardon, G. Aharonian, S. Gambarotta, G. P. A. Yap, O *rganometallics* **2002**, *21*, 786.

[7] a) M. Kooistra, Q. Knijnenburg, J. M. M. Smits, A. D. Horton, P. H. M. Budzelaar, A. W. Gal, *Angew. Chem.* **2001**, *113*, 4855; *Angew. Chem. Int. Ed.* **2001**, *40*, 4719; b) V. C. Gibson, M. Humphries, K. Tellmann, D. Wass, A. J. P. White, D. J. Williams, *Chem. Commun.* **2001**, 2252.

[8] Geometry optimizations of the minima and transition states were performed with the GAMESS-UK package[9] using the B3LYP hybrid density functional[10] with the split-valence 3-21G basis set.[11] Geometries were optimized without constraints. Figure S1 compares calculated and observed bond lengths (see Supporting Information).

[9] GAMESS-UK is a package of ab initio programs written by M. F. Guest, J. H. van Lenthe, J. Kendrick, K. Schoffel, and P. Sherwood, with contributions from R. D. Amos, R. J. Buenker, H. J. J. van Dam, M. Dupuis, N. C. Handy, I. H. Hillier, P. J. Knowles, V. Bonacic-Koutecky, W. von Niessen, R. J. Harrison, A. P. Rendell, V. R. Saunders, A. J. Stone, D. J. Tozer, A. H. de Vries. The package is derived from the original GAMESS code attributed to M. Dupuis, D. Spangler, J. Wendoloski, NRCC Software Catalog, Vol. 1, Program No. QG01 (GAMESS), **1980**.

  0044-8249/02/4120-3875 $ 20.00+.50/0

[10] A. D. Becke, *J. Chem. Phys.* **1993**, *98*, 5648; C. Lee, W. Yang, R. G. Parr, *Phys. Rev. B* **1988**, *37*, 785; B. Miehlich, A. Savin, H. Stoll, H. Preuss, *Chem. Phys. Lett.* **1989**, *157*, 200.

[11] J. S. Binkley, J. A. Pople, W. J. Hehre, *J. Am. Chem. Soc.* **1980**, *102*, 939; M. S. Gordon, J. S. Binkley, J. A. Pople, W. J. Pietro, W. J. Hehre, *J. Am. Chem. Soc.* **1982**, *104*, 2797; M. J. Frisch, J. A. Pople, J. S. Binkley, *J. Chem. Phys.* **1984**, *80*, 3265, and references therein; K. D. Dobbs, W. J. Hehre, *J. Comput. Chem.* **1986**, *7*, 359; K. D. Dobbs, W. J. Hehre, *J. Comput. Chem.* **1987**, *8*, 861, 880.

Room-Temperature Synthesis in Acidic Media of Large-Pore Three-Dimensional Bicontinuous Mesoporous Silica with *Ia*3*d* Symmetry**

Xiaoying Liu, Bozhi Tian, Chengzhong Yu, Feng Gao, Songhai Xie, Bo Tu, Renchao Che, Lian-Miao Peng, and Dongyuan Zhao*

Since the discovery of a new family of mesoporous silicate materials, denoted M41S and including MCM-41, MCM-48, and MCM-50, by researchers at Mobil,[1] major developments have been made in this field. A great variety of mesostructures has been obtained, including mesoporous silica, metal oxides, metals, carbon, and hybrid organosilicates.[2] Up to now, the main research efforts have concentrated on the MCM-41 silica structure, which consists of a hexagonal packing of one-dimensional (1D) channels (*p*6*mm*), and fewer investigations have been reported on mesoporous MCM-48, which has a 3D bicontinuous mesostructure (*Ia*3*d*). This may result from the small domain of this cubic phase (*Ia*3*d*) of MCM-48 in phase diagrams. Several methodologies have been developed for the syntheses of mesoporous silica MCM-48 by using a cationic alkylammonium surfactant,[1,3] mixed cationic/anionic surfactants,[4] or cationic/nonionic surfactants as templates.[5] Generally, these syntheses were carried out under the severe conditions of high-temperature ($\geq 100\,^{\circ}C$) hydrothermal synthesis in alkaline aqueous media. Relatively expensive ionic surfactants were employed, and the resulting mesostructures have a limited range of small pore sizes (pore diameter 1.5–4.5 nm). These restrictions may limit the potential applications of 3D bicontinuous mesoporous materials as adsorbents, separators, and catalysts.

[*] Prof. D. Zhao, X. Liu, B. Tian, Dr. C. Yu, F. Gao, S. Xie, Prof. B. Tu
Laboratory of Molecular Catalysis and Innovative Materials
Department of Chemistry, Fudan University
Shanghai 200433 (China)
Fax: (+86) 21-6564-1740
E-mail: dyzhao@fudan.edu.cn

R. Che, Prof. L.-M. Peng
Beijing Laboratory of Electron Microscopy, Institute of Physics
Chinese Academy of Sciences, Beijing 100083 (China)

[**] This work was supported by the National Natural Science Foundation of China (Grants No. 29925309 and 20173012), Chinese Ministry of Education, Shanghai NanoTech Center (0152nm029) and State Key Basic Research Program of PRC (2001CB610505).

Supporting information for this article is available on the WWW under http://www.angewandte.org or from the author.

Here we report the synthesis of large-pore 3D bicontinuous mesoporous silica (designated FDU-5) at room temperature in acidic media by using a commercial nonionic triblock copolymer as template and an organosiloxane or organic compound as additive. To the best of our knowledge, this is the first preparation of *Ia*3*d* mesostructured material at room temperature under acidic conditions. The FDU-5 products have uniform large pores (4.5–9.5 nm). Such mesoporous materials with large 3D bicontinuous pores could have applications in sorption and transport, especially of large molecules.

Large-pore 3D bicontinuous mesoporous FDU-5 was synthesized at room temperature in ethanol solution by a solvent-evaporation method. Triblock poly(ethylene oxide)-*b*-poly(propylene oxide)-*b*-poly(ethylene oxide) copolymer ($EO_{20}PO_{70}EO_{20}$, P123) was used as template, tetraethyl orthosilicate (TEOS) as silica source, and a small amount of 3-mercaptopropyltrimethoxysilane (MPTS), benzene, or a benzene derivative (methyl-, ethyl-, dimethyl-, or trimethylbenzene) as additive.

Transmission electron microscopy (TEM) images and corresponding Fourier diffractograms recorded along the [100], [111], [110], and [331] directions of calcined FDU-5 silica prepared with P123 as template and MPTS as additive in acidic medium at room temperature are shown in Figure 1. These images clearly show that the products have large domains of ordered 3D bicontinuous mesostructure. The two principal directions displaying continuous pores are [100] and [111] (Figure 1 a,b), and two types of hexagonally packed dots with different sizes and darknesses (Figure 1 b) are clearly observed. The images shown in Figure 1 are beautiful representative packing patterns for bicontinuous cubic mesostructures (*Ia*3*d*).[6,7] The cell parameter *a* calculated from these TEM images is 18.0 nm. On the basis of these TEM

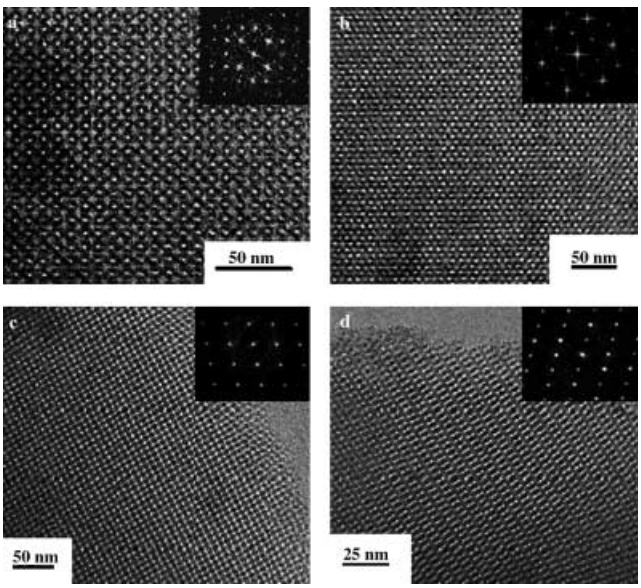

Figure 1. TEM images and corresponding Fourier diffractograms of calcined FDU-5 prepared at room temperature under acidic conditions with triblock copolymer P123 as template and MPTS as additive. The images were recorded along the directions [100] (a), [111] (b), [110] (c), and [331] (d).

  0044-8249/02/4120-3876 $ 20.00+.50/0